CHAPTER III

RESULTS

1. Metaphase karyotype identification

The results of investigations of F_1- and/or F_2-progenies of 3, 4 and 89 isolines of *An. aconitus* strains from Mae Hong Son, Phetchaburi and Chiang Mai provinces revealed the two forms of metaphase karyotypes, *i.e.*, Form B (X_1, X_2, Y_2), and C (X_1, X_2, Y_3). Form B was obtained from 4 and 48 isolines of Phetchaburi and Chiang Mai strains, respectively, and Form C was recovered from 3 and 41 isolines of Mae Hong Son and Chiang Mai strains, respectively. It was interesting to note that *An. aconitus* Form A (X_1, X_2, Y_1) collected from Maetang district, Chiang Mai province, and Sadao district, Songkla province in October 1983, and subsequently reported by Baimai *et al.* (1996a), was not found in this study. The Y_1-chromosome is small submetacentric, the Y_2-chromosome is medium submetacentric having an extra block of heterochromatin added into each arm of the Y_1-chromosome, and the Y_3-chromosome is clearly large submetacentric arised from the Y_2-chromosome by addition of an extra block of heterochromatin on the long arm. The X_1-chromosome is metacentric, in which the X_2-chromosome is large submetacentric arised from the X_1-chromosome by addition of a major block of heterochromatin (Figure 3).

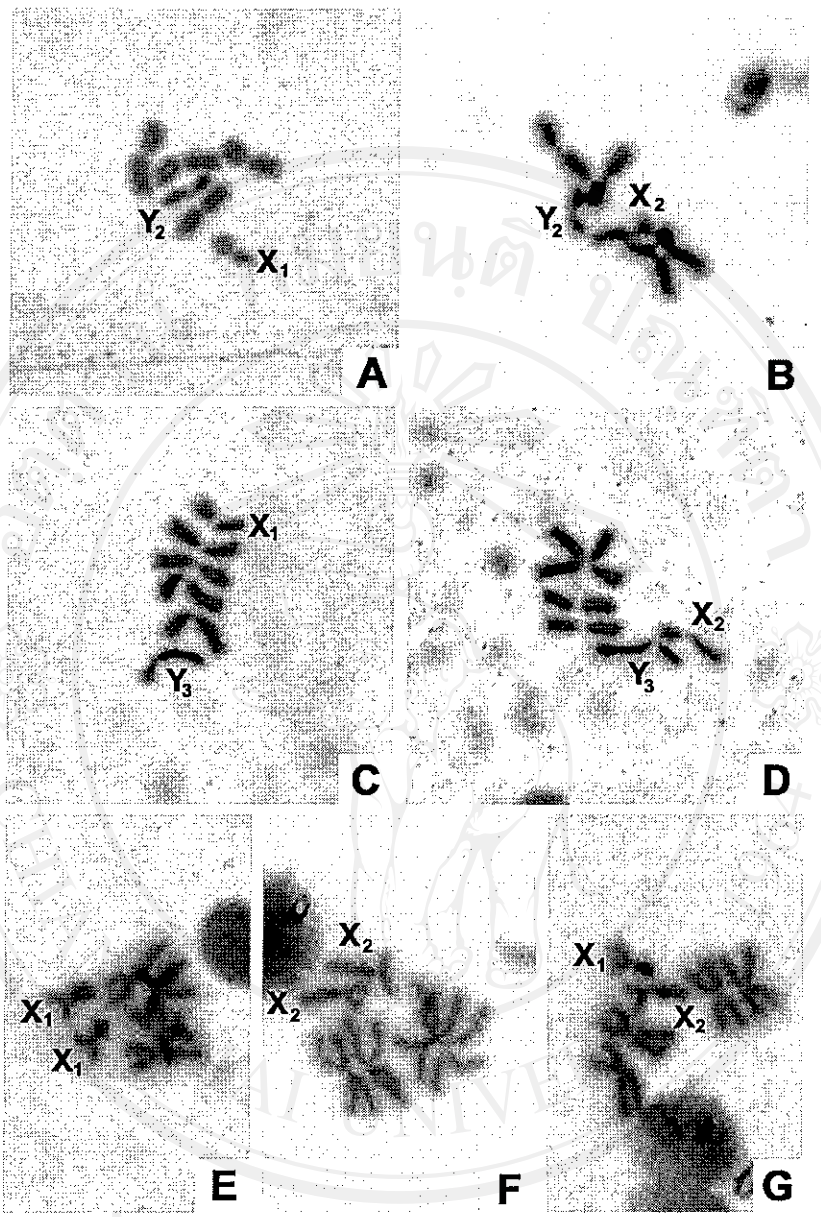

Figure 3. Metaphase karyotypes of *An. aconitus* Form B and C (Giemsa staining). Testis chromosomes; Form B: (A) Chiang Mai strain, showing X_1, Y_2-chromosomes; (B) Phetchaburi strain, showing X_2, Y_2-chromosomes; Form C: (C) Chiang Mai strain, showing X_1, Y_3-chromosomes; (D) Mae Hong Son strain, showing X_2, Y_3-chromosomes. Ovary chromosomes: (E) showing homozygous X_1, X_1-chromosomes, (F) showing homozygous X_2, X_2-chromosomes, (G) showing heterozygous X_1, X_2-chromosomes. Note, all types of X-chromosomes were found in all forms and strains of *An. aconitus*.

2. Morphometric and morphological studies of eggs, larvae, pupae and adults under light and/or scanning electron microscopy

2.1 Morphometric and morphological studies of larvae, pupae and adults under light microscopy

The results of comparative setal branching on 4th instar larvae (2-C, 3-C, 4-C, 3-T, O-IV, O-V, O-VI) between *An. aconitus* Form B and C demonstrated no statistically significant difference ($P > 0.05$) (Table 3). Regarding the results of comparative setal branching on pupal skins (O-III-VII, 4-IV, 7-III-IV) between *An. aconitus* Form B and C, no statistically significant difference was revealed ($P > 0.05$) (Table 4).

Comparisons of specific diagnostic characters in adult females (palpus, proboscis, wing, leg) between *An. aconitus* Form B and C demonstrated no statistically significant difference ($P > 0.05$) (Table 5). Nonetheless, *An. aconitus* Form B tended to exhibit morphological variation in adults that were compatible to *An. minimus* A. The variable characteristics were an entirely dark proboscis (10.52%, 4/38), presence of a presector pale spot on both wings (10.52%, 4/38) and absence of a median pale spot on vein R_2 in both wings (5.26%, 2/38).

When comparing the mean numbers of coeloconic sensillae segment by segment of the flagellum for *An. aconitus* Form B and C, the coeloconic sensillae were present in Form B from segment 1-12, with only one mosquito shown on segment 10 and 11 (1/38). In Form C, no mosquitoes were present on segment 10 and 11 (0/32) (Table 6). Comparative mean numbers of coeloconic sensillae per antenna, palpal ratios, and wing dimensions of *An. aconitus* Form B and C were found not statistically different ($P > 0.05$) (Table 7). The combined characteristics plotted on a

scatter diagram between coeloconic sensillae and palpal ratios of *An. aconitus* Form B and C could be separated at a 20% level (Figure 4).

Table 3. Setal branching on 4th instar larvae of *An. aconitus* Form B and C.

Characters	Form B*	Form C**
	$\bar{X} \pm SD$ (range)	$\bar{X} \pm SD$ (range)
2-C		
L	7.58 ± 3.49 (0-15)	9.16 ± 3.29 (1-14)
R	7.68 ± 3.42 (0-15)	8.84 ± 3.08 (0-14)
3-C		
L	3.66 ± 2.13 (0-7)	3.28 ± 1.67 (0-8)
R	3.13 ± 1.95 (0-7)	4.12 ± 1.86 (1-9)
4-C		
L	3.00 ± 0.99 (1-6)	3.03 ± 1.00 (1-5)
R	3.03 ± 0.79 (1-5)	3.25 ± 0.72 (2-5)
3-T		
L	11.82 ± 2.66 (8-18)	11.84 ± 2.10 (8-15)
R	11.82 ± 2.67 (6-18)	12.00 ± 2.30 (8-16)
O-IV		
L	1.24 ± 0.49 (1-3)	1.41 ± 0.50 (1-2)
R	1.32 ± 0.53 (1-3)	1.22 ± 0.42 (1-2)
O-V		
L	1.42 ± 0.50 (1-2)	1.50 ± 0.51 (1-2)
R	1.45 ± 0.50 (1-2)	1.47 ± 0.51 (1-2)
O-VI		
L	1.34 ± 0.48 (1-2)	1.50 ± 0.51 (1-2)
R	1.61 ± 0.64 (1-3)	1.53 ± 0.51 (1-2)

*38 specimens examined, ** 32 specimens examined; L = Left; R = Right

Table 4. Setal branching on pupal skins of *An. aconitus* Form B and C.

Characters	Form B* $\bar{X} \pm SD$ (range)	Form C* $\bar{X} \pm SD$ (range)
O-III		
L	1.03 ± 0.18 (1-2)	1.13 ± 0.35 (1-2)
R	1.07 ± 0.25 (1-2)	1.20 ± 0.41 (1-2)
O-IV		
L	1.10 ± 0.31 (1-2)	1.13 ± 0.35 (1-2)
R	1.20 ± 0.41 (1-2)	1.17 ± 0.46 (1-2)
O-V		
L	1.17 ± 0.46 (1-3)	1.03 ± 0.18 (1-2)
R	1.20 ± 0.41 (1-2)	1.13 ± 0.35 (1-2)
O-VI		
L	1.17 ± 0.38 (1-2)	1.20 ± 0.41 (1-2)
R	1.07 ± 0.25 (1-2)	1.13 ± 0.34 (1-2)
O-VII		
L	1.00 ± 0.00 (1)	1.00 ± 0.00 (1)
R	1.03 ± 0.18 (1-2)	1.10 ± 0.31 (1-2)
4-IV		
L	1.97 ± 0.41 (1-5)	2.10 ± 0.40 (1-4)
R	2.00 ± 0.26 (1-4)	2.03 ± 0.41 (1-4)
7-III		
L	3.77 ± 0.68 (2-5)	3.87 ± 0.57 (1-5)
R	3.83 ± 0.59 (1-5)	3.60 ± 0.97 (2-4)
7-IV		
L	1.93 ± 0.37 (1-4)	2.00 ± 0.37 (1-5)
R	1.96 ± 0.32 (1-4)	2.03 ± 0.32 (1-3)

* 30 specimens examined; L = Left; R = Right

Table 5. Comparative adult female characters of *An. aconitus* Form B and C.

Characters	Form B* No. (%)	Form C** No. (%)
Palpus		
Subapical dark band present (both)	25 (65.79)	23 (71.88)
Subapical dark band absent (one)	5 (13.16)	6 (18.75)
Subapical dark band absent (both)	8 (21.05)	3 (9.38)
Proboscis		
Entirely pale on distal 0.3-0.5	23 (60.53)	20 (62.50)
Partially pale on distal 0.3	11 (28.95)	12 (37.50)
Entirely dark	4 (10.52)	0 (0)
Wing		
Humeral pale spot absent (both)	36 (94.74)	31 (96.88)
Humeral pale spot present (one)	1 (2.63)	1 (3.12)
Humeral pale spot present (both)	1 (2.63)	0 (0)
Presector pale spot absent (both)	33 (86.84)	32 (100)
Presector pale spot present (one)	1 (2.63)	0 (0)
Presector pale spot present (both)	4 (10.52)	0 (0)
Median pale spot on vein R_2 present (both)	34 (89.47)	30 (93.75)
Median pale spot on vein R_2 absent (one)	2 (5.26)	2 (6.25)
Median pale spot on vein R_2 absent (both)	2 (5.26)	0 (0)
R base without dark scales (both)	38 (100)	32 (100)
Vein 1A with 3 dark spots (both)	35 (92.11)	30 (93.75)
Vein 1A with 2 dark spots (one)	1 (2.63)	1 (3.12)
Vein 1A with 2 dark spots (both)	2 (5.26)	1 (3.12)
Vein 1A with pale fringe (both)	30 (78.95)	24 (75.00)
Vein 1A with dark fringe (one)	5 (13.16)	4 (12.50)
Vein 1A with dark fringe (both)	3 (7.89)	4 (12.50)
Leg		
Fore tarsi with pale band at joints (both)	38 (100)	32 (100)

*38 specimens examined, **32 specimens examined

Table 6. Mean distribution of coeloconic sensillae on antennal segments of *An. aconitus* Form B (n = 38) and C (n = 32).

Antennal segment	*An. aconitus* Form	
	B	C
	$\bar{X}$ ± SD (range)	$\bar{X}$ ± SD (range)
1	4.26 ± 1.06 (3-6)	4.25 ± 1.34 (2-6)
2	4.76 ± 1.02 (3-7)	4.94 ± 0.98 (3-8)
3	4.87 ± 0.81 (3-6)	5.13 ± 0.91 (3-7)
4	4.76 ± 0.71 (3-6)	4.47 ± 0.76 (3-6)
5	4.08 ± 0.85 (2-6)	4.09 ± 0.82 (2-6)
6	3.61 ± 1.00 (2-6)	3.69 ± 0.78 (2-5)
7	2.74 ± 0.83 (1-4)	2.19 ± 1.09 (0-4)
8	0.71 ± 0.65 (0-2)	0.94 ± 0.72 (0-2)
9	0.24 ± 0.49 (0-2)	0.16 ± 0.37 (0-1)
10	0.03 ± 0.16 (0-1)	0 (0)
11	0.05 ± 0.23 (0-1)	0 (0)
12	0.03 ± 0.16 (0-1)	0.03 ± 0.18 (0-1)
13	0 (0)	0 (0)

Table 7. Comparative mean numbers of coeloconic sensillae per antenna, palp ratios and wing dimensions of *An. aconitus* Form B (n = 38) and C (n= 32).

An. aconitus Form	Average coeloconic sensillae per antenna (range)*	Average palp ratio (range)**	Wing dimensions (range)	
			Length (mm)***	Width (mm)****
B	30.13 ± 4.95 (20-39)	0.74 ± 0.05 (0.56-0.83)	1.31 ± 0.04 (1.19-1.37)	0.49 ± 0.02 (0.43-0.52)
C	29.88 ± 4.26 (21-39)	0.75 ± 0.04 (0.64-0.85)	1.30 ± 0.06 (1.54-1.37)	0.48 ± 0.02 (0.43-0.50)

*t = 0.541, P > 0.05
**t = 0.421, P > 0.05
***t = 0.177, P > 0.05
****t = 0.499, P > 0.05

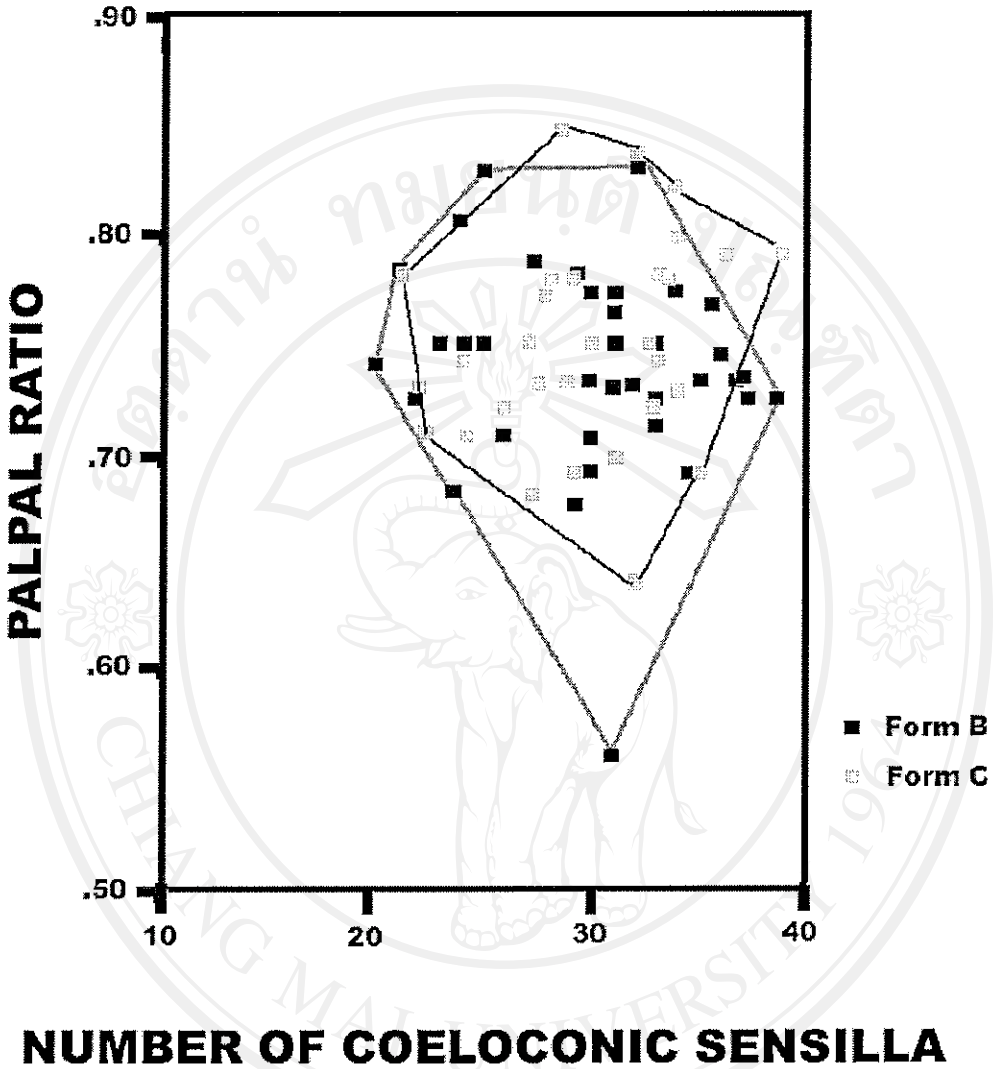

Figure 4. Scatter diagram of coeloconic sensilla and palpal ratios in *An. aconitus* Form B (■) and C (▣)

2.2 Scanning electron microscopy

2.2.1. Morphometric measurements and counts of float ribs and tubercles

Details of morphometric measurements and counts of float ribs and tubercles are shown in Table 8. Statistical analysis of egg dimensions at various sites, using the F-test for all tests and Kruskal-Wallis test for width including floats and number of posterior tubercles on deck, demonstrated that in most cases, *i.e.*, entire length, width including floats, float length, number of float ribs and number of anterior tubercles, exhibited no significant differences ($P > 0.05$) among the three strains of *An. aconitus* Form B and C. Intraspecific variations with respect to the none correlation among the three strains of two karyotypic forms of *An. aconitus* were float width [36.77 ± 2.30 μm (Form C: Chiang Mai strain) = 38.49 ± 2.78 μm (Form B: Chiang Mai strain) = 39.06 ± 2.37 μm (Form B: Phetchaburi strain) > 32.40 ± 3.52 μm (Form C: Mae Hong Son strain) ($F = 11.73$, $P < 0.05$)] and number of posterior tubercles on deck [2.40 ± 0.52 (Form B: Phetchaburi strain) = 2.70 ± 0.82 (Form B: Chiang Mai strain) < 3.10 ± 0.32 (Form C: Chiang Mai strain) = 3.20 ± 0.42 (Form C: Mae Hong Son strain) ($H = 11.43$, $P < 0.05$)].

Table 8. Morphometric measurements and counts of float ribs and tubercles of eggs of *An. aconitus* Form B (Chiang Mai and Phetchaburi strains) and C (Chiang Mai and Mae Hong Son strains).

Experiments	Eggs of *An. aconitus* Form*			
	B		C	
	CM	PB	CM	MS
Measurements				
Entire length	361.99 ± 24.38 (334.80-404.20)	367.32 ± 19.22 (337.53-395.87)	359.61 ± 25.24 (329.19-400.03)	370.03 ± 21.66 (312.52-389.61)
Width including floats	141.10 ± 14.90 (126.09-179.18)	137.93 ± 16.58 (112.51-166.68)	142.51 ± 4.30 (137.51-150.01)	136.68 ± 5.57 (129.18-145.85)
Float length	309.05 ± 15.39 (280.45-331.28)	322.11 ± 9.63 (302.11-331.28)	316.48 ± 19.31 (279.19-337.53)	313.57 ± 18.77 (270.85-335.44)
Float width	38.49 ± 2.78 (34.78-43.75)	39.06 ± 2.37 (35.42-43.75)	36.77 ± 2.30 (33.34-39.59)	32.40 ± 3.52 (25.00-37.50)
Counts				
No. float ribs	16.90 ± 1.37 (15-19)	15.50 ± 1.51 (13-18)	16.40 ± 1.78 (13-19)	15.60 ± 1.26 (14-17)
No. anterior tubercles	2.40 ± 0.52 (2-3)	2.70 ± 0.48 (2-3)	3.00 ± 0.47 (2-4)	2.90 ± 0.32 (2-3)
No. posterior tubercles	2.70 ± 0.82 (2-4)	2.40 ± 0.52 (2-3)	3.10 ± 0.32 (3-4)	3.20 ± 0.42 (3-4)

Mosquito strain; CM: Chiang Mai, MS: Mae Hong Son, PB: Phetchaburi.
*Ten samples for each strain.
Measurements in μm ± SD, range in parenthesis.

2.2.2 Eggs topography of three strains of *An. aconitus* Form B and C

The morphological feature and exochorionic sculpturing of the three egg strains of *An. aconitus* Form B (Chiang Mai and Phetchaburi strains) and C (Chiang Mai and Mae Hong Son strains) were generally similar (Figures 5-22), and no account of form specific characteristics that could be used to differentiate and/or characterize the forms under SEM. The eggs were boat-shaped, with a somewhat broader anterior or head-end (Figures 5-7). Viewed laterally, the contour of the entire egg was slightly concave on the morphologically dorsal surface and convex on the ventral surface. The middle region of each egg side was dominated by a float with approximately 16 (13-18) (Form B: Phetchaburi strain), 17 (15-19) (Form B: Chiang Mai strain), 16 (13-19) (Form C: Chiang Mai strain) and 16 (14-17) ribs (Form C: Mae Hong Son strain). Viewed dorsally, there was a bare area, which was surrounded by the two longitudinal bands of a sclerotized ridge-like frill; this bare area is called the deck. The deck was continuous for the whole length of the egg and slightly constricted near the midline. Large-lobed tubercles that ranged from 2-4 in number were at each end of the egg on the ventral surface (Figures 8, 9). Large-lobed tubercles on the anterior and posterior ends were rosette-shaped, giving rise to 7-9 lateral lobes, and surrounded by a sclerotized ridge and raised border (Figure 10). The tubercles on either the deck (Figure 11) or in areas covered by floats (observed from detached-float specimens) (Figures 12-14) were irregularly jagged and surrounded by other much smaller, irregular tubercles. The cluster of tubercles adjacent to the detachment point of the float more or less formed a wavy border, and were apparently larger than other tubercles on the area covered by the float. The outer chorionic tubercles between the frill and detachment point of the float, were completely covered

with a membrane-like sheet (Figure 15). In a torn membrane-like sheet specimen, the tubercles were of an irregular base and a flattened-surface (Figure 16). The inner surface of the frill was of a sclerotized, ridged-like texture and marked by picket like-ribs (Figure 17); the outer surface was smooth with a parallel brick-like texture along its entire length (Figure 18). At the anterior end, the micropylar orifice could be seen clearly. It was surrounded by a smooth collar that had an irregular outer margin and 4-6 spurs that extended radially toward the central orifice. One small central knob was seen clearly in unfertilized eggs (Figure 19). Outer chorionic tubercles were present on the entire egg surface, except on the deck and the areas covered by floats. Tubercles, seen all over the eggs (lateral, dorsal, ventral surfaces), had an irregular base, with their surface partially covered with a membrane-like sheet at the anterior third and posterior third of the eggs (Figure 20), and almost completely covered in the middle (Figure 21). On observation of the torn membrane-like sheet specimens, the tubercles were seen clearly to have an irregular base and flattened-surface; these tubercles were arranged singularly (Figure 22).

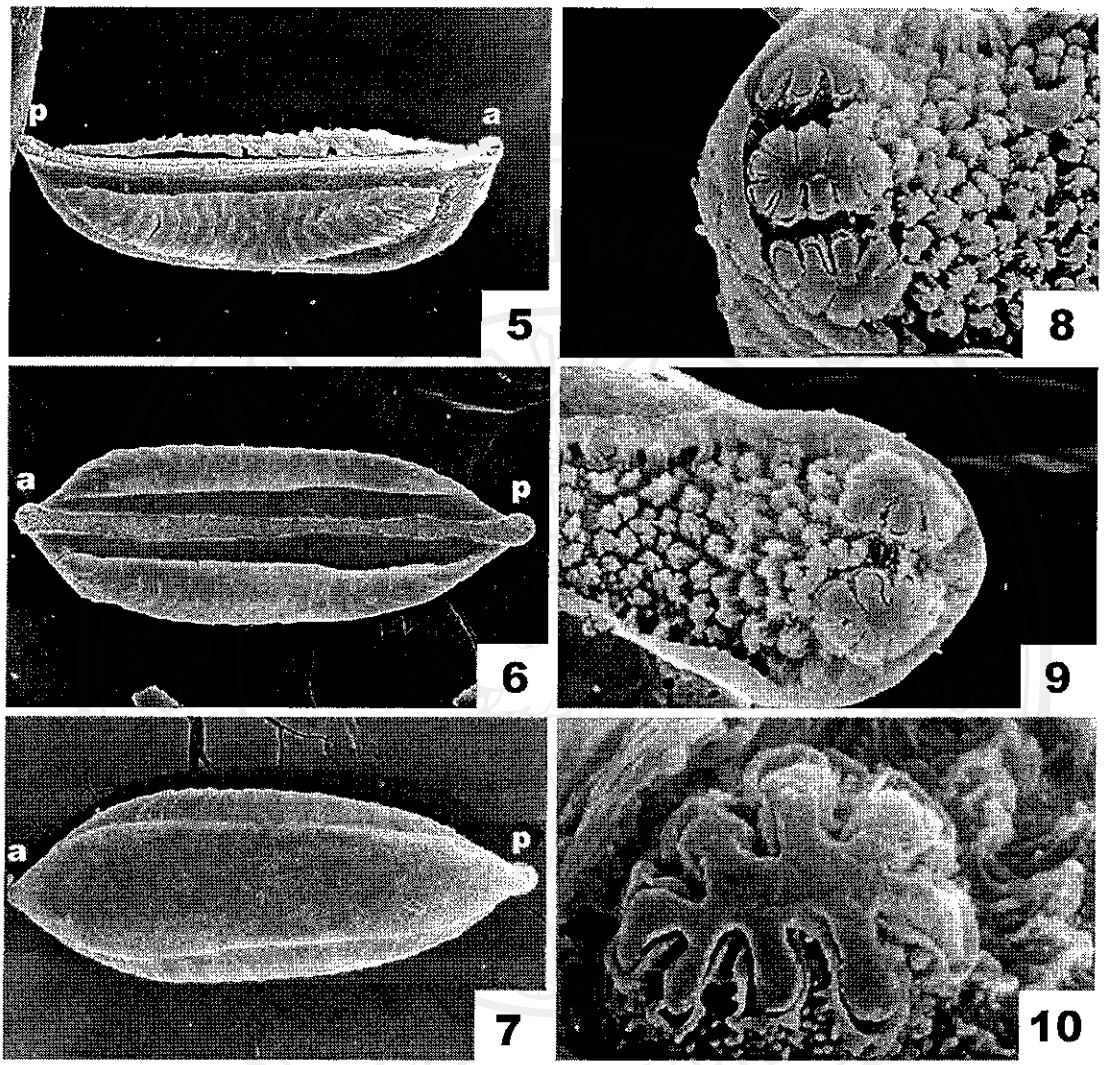

Figure 5-10. Whole eggs: (5) Lateral aspect, anterior end (a), posterior end (p) (x 270), (6) Dorsal aspect, anterior end (a), posterior end (p) (x 270), (7) Ventral aspect, anterior end (a), posterior end (p) (x 270). (8) Anterior end, showing irregularly jagged tubercles on the deck and three large, rosette-shaped tubercles (x 3,500). (9) Posterior end, showing irregularly jagged tubercles on the deck and two large, rosette-shape tubercles (x 3,500). (10) A higher magnification of the large, rosette-shaped tubercle, surrounded by a sclerotized ridge and raised border (x 10,000).

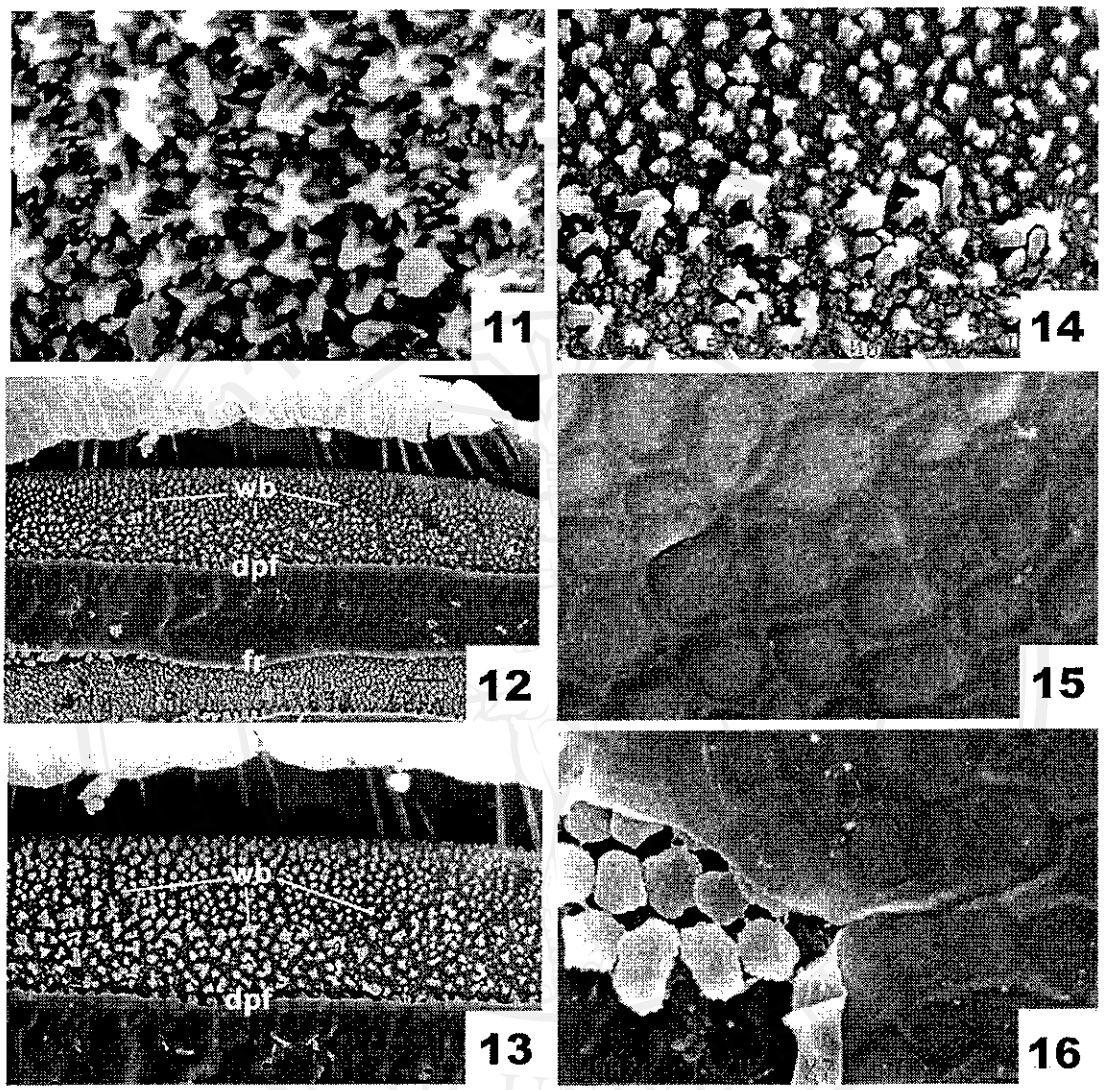

Figures 11-16. (11) A higher magnification of the irregularly jagged tubercles on the deck (x 12,000). (12) Irregularly jagged tubercles on the deck and area covered by the float, and outer chorionic tubercles covered with a membrane-like sheet between the frill (fr) and detachment point of the float (dpf). Note, that the cluster of tubercles adjacent to the detachment point of the float more or less form a wavy border (wb) (x 850). (13) A higher magnification of the irregularly jagged tubercles on the area covered by the float, and outer chorionic tubercles covered with a membrane-like sheet between the frill and detachment point of the float (x 1,500). (14) A higher magnification of the irregularly jagged tubercles on the area covered by the float (x 5,000). (15) A higher magnification of the outer chorionic tubercles covered with a membrane-like sheet between the frill and detachment point of the float (x 8,000). (16) Outer chorionic tubercles from the torn membrane-like sheet between the frill and detachment point of the float (x 540).

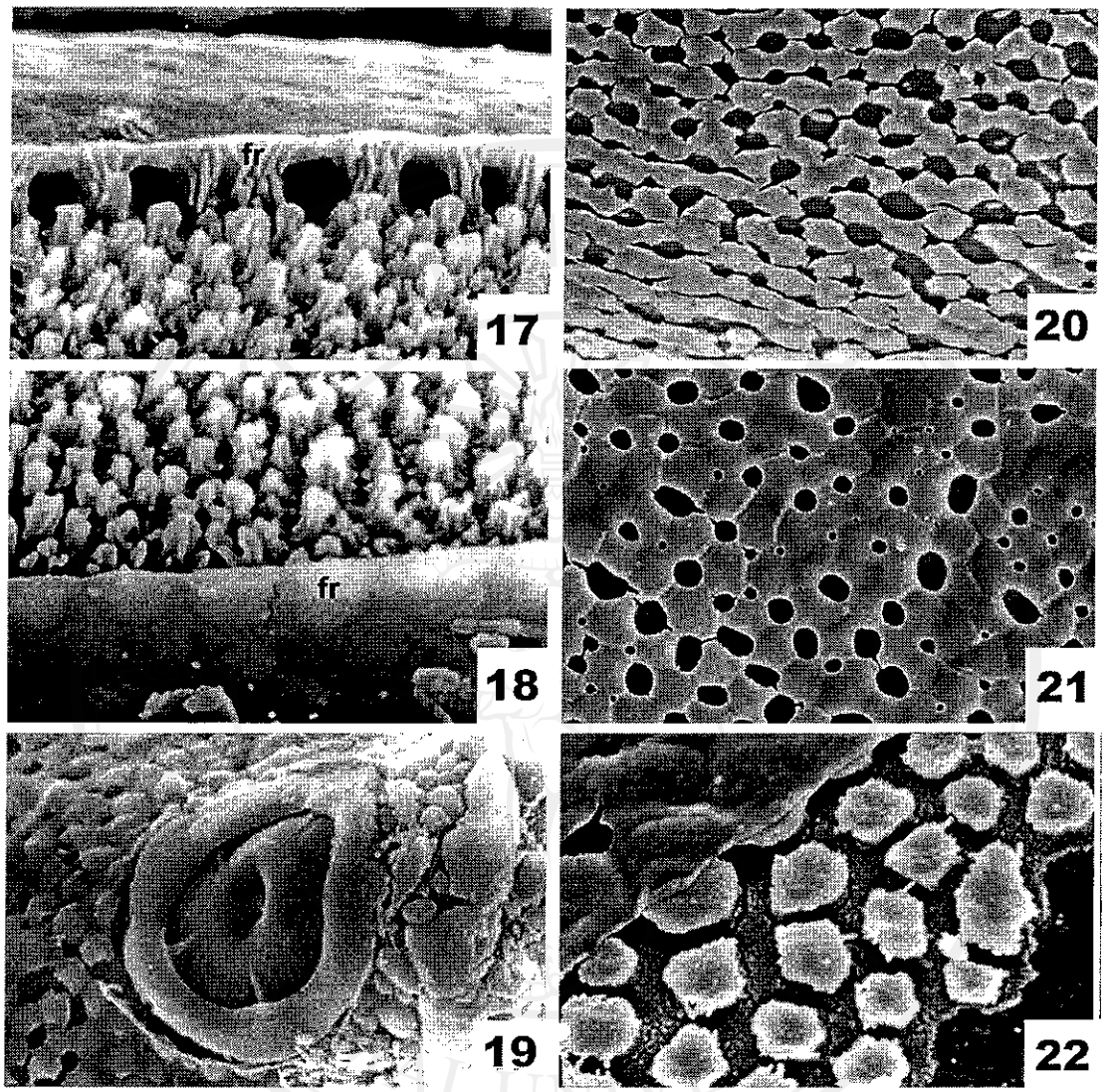

Figures 17-22. (17) The inner surface of the frill (fr), showing its sclerotized, ridge-like texture with picket-like ribs (x 8,000). (18) The outer surface of the frill (fr), showing its smooth surface and parallel brick-like texture along its entire length (x 8,000). (19) The anterior end, showing the micropylar orifice surrounded by a smooth collar with an irregular outer margin (x 3,700). (20) Outer chorionic tubercles at the anterior third of the egg, showing irregular bases partially covered with a membrane-like sheet (x 3,500). (21) Outer chorionic tubercles in the middle of the egg, showing irregular bases that were almost completely covered with a membrane-like sheet (x 3,500). (22) Outer chorionic tubercles from the torn membrane-like sheet in the middle of the egg, showing irregular bases and flattened-surface (x 7,000).

3. Ovarian nurse cell polytene chromosome investigation

Only *An. aconitus* Form B and Form C were obtained from this study, therefore, the standard homozygote of ovarian nurse cell polytene chromosomes were prepared from F_1- and/or F_2-progenies of *An. aconitus* Form B. Standard map and/or zone division of the five arms of chromosomes (20 complete sets of chromosomes, one set from each isoline) were based on the former reports of *An. aconitus* salivary gland polytene chromosomes (Sharma *et al.*, 1980) and followed the convention of White *et al.* (1975) in *Anopheles*. Thus, the ovarian nurse cell polytene chromosomes of *An. aconitus* Form B were divided into a total of 46 zones, numbered from 1 to 46. In the map presented (Figure 23), there are 6 zones (1-6) in chromosome X, 13 zones (7-19) in chromosome 2R (2), 9 zones (20-28) in chromosome 2L (3), 9 zones (29-37) in chromosome 3R (4), and 9 zones (38-46) in chromosome 3L (5). When comparing bands on the same arm of 3 (Form C: Mae Hong Son strain), 4 (Form B: Phetchaburi strain), and 20 (Form C: Chiang Mai strain) complete sets of chromosomes to standard chromosomes, no major chromosomal rearrangements that related to the karyotype variations were demonstrated.

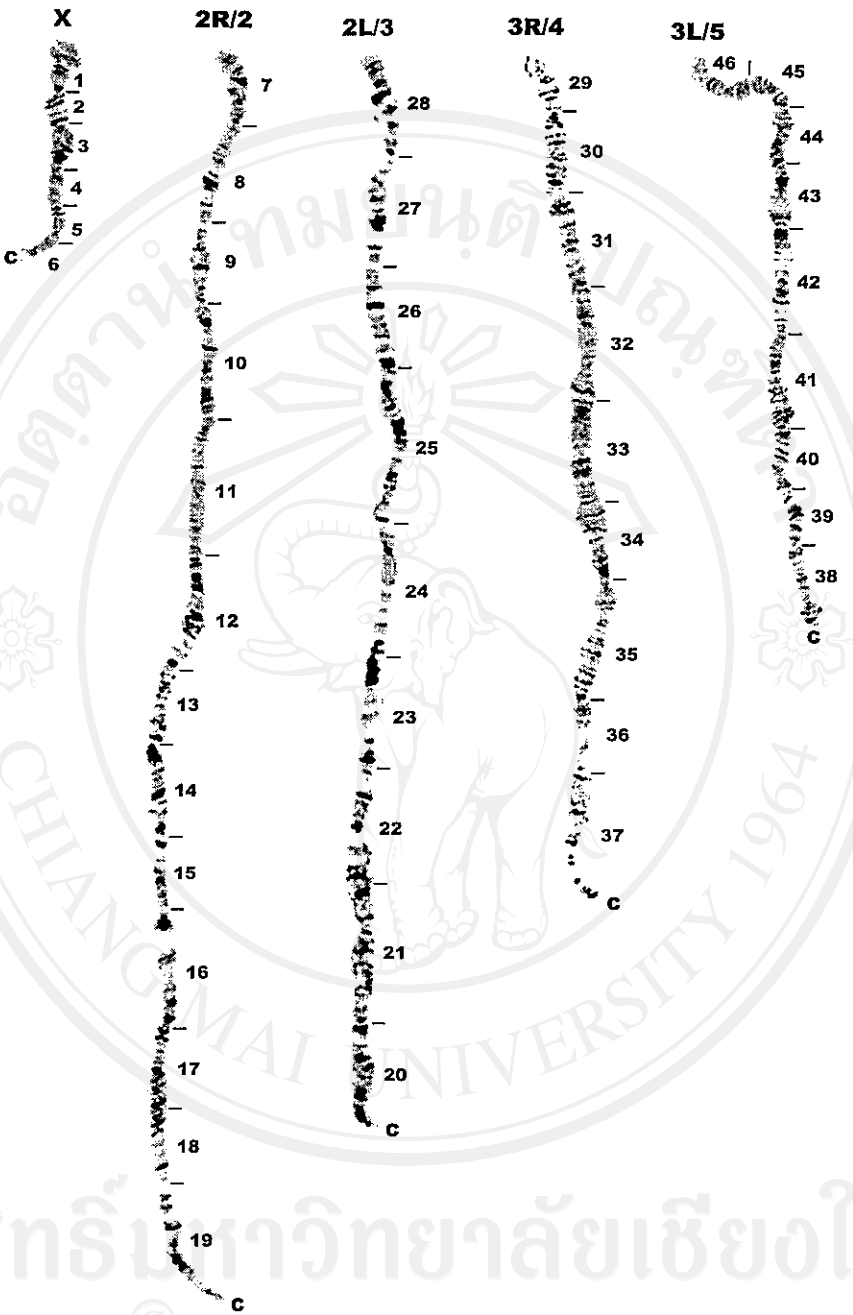

Figure 23. Standard map of ovarian nurse cell polytene chromosomes of *An. aconitus* Form B (Chiang Mai strain).

4. Isoenzyme study

Sixteen out of nineteen isoenzymes could be detected and analyzed. Details of allelic frequencies are shown in Table 9, 10 and Figure 24, 25. The results of investigations on allelic frequencies of 4th instar larvae and adult females of 3 (Form C: Mae Hong Son strain), 4 (Form B: Phetchaburi strain), 41 (Form C: Chiang Mai strain), and 48 (Form B: Chiang Mai strain) isolines indicated that *An. aconitus* Form B and C of all strains had similar allelic frequencies observed at 10 isoenzymes 16 loci in 4th instar larvae, and 11 isoenzymes 13 loci in adult females of sympatric *An. aconitus* Form B and C (Chiang Mai strain), and allopatric *An. aconitus* Form B (Phetchaburi strain) and C (Mae Hong Son strain)

Table 9. Allelic frequencies (allele numbers) observed at 10 isoenzymes 16 loci in 4th instar larvae of *An. aconitus* Form B (Chiang Mai and Phetchaburi strains) and C (Chiang Mai and Mae Hong Son strains).

No.	Loci	Allele	*An. aconitus* Form			
			B		C	
			CM	PB	CM	MS
1	*Est-5*	100	0.78 (56)	1.00 (6)	0.89 (52)	0.33 (2)
		104	0.22 (16)	0 (0)	0.11 (6)	0.67 (4)
2	*Idh-2*	100	0.80 (16)	1.00 (6)	0.83 (15)	1.00 (6)
		105	0.15 (3)	0 (0)	0.11 (2)	0 (0)
		108	0.05 (1)	0 (0)	0.06 (1)	0 (0)
3	*Lap-2*	100	0.92 (22)	1.00 (6)	0.83 (10)	1.00 (6)
		102	0.08 (2)	0 (0)	0.17 (2)	0 (0)
4	*Lap-3*	100	1.00 (44)	1.00 (6)	1.00 (26)	1.00 (6)
5	*Lap-4*	100	1.00 (44)	1.00 (6)	1.00 (26)	1.00 (6)
6	*Lap-5*	100	1.00 (44)	1.00 (6)	1.00 (26)	1.00 (6)
7	*Lap-6*	100	0.73 (32)	1.00 (6)	0.83 (20)	1.00 (6)
		102	0.27 (12)	0 (0)	0.17 (4)	0 (0)
8	*Ldh-1*	100	1.00 (16)	1.00 (6)	1.00 (20)	1.00 (6)
9	*Ldh-2*	98	0.11 (6)	1.00 (6)	0.04 (2)	1.00 (6)
		100	0.89 (48)	0 (0)	0.96 (46)	0 (0)
10	*Me*	100	1.00 (24)	1.00 (6)	1.00 (12)	1.00 (6)
11	*Gpi*	100	0.82 (18)	1.00 (6)	0.78 (14)	1.00 (6)
		105	0.18 (4)	0 (0)	0.22 (4)	0 (0)
12	*Gpd*	100	0.96 (25)	1.00 (6)	1.00 (14)	1.00 (6)
		102	0.04 (1)	0 (0)	0 (0)	0 (0)
13	*Acp*	95	0.25 (2)	0.75 (6)	0.29 (4)	0.67 (4)
		100	0.75 (6)	0.25 (2)	0.43 (6)	0.33 (2)
		102	0 (0)	0 (0)	0.28 (4)	0 (0)
14	*Alp*	98	0.40 (4)	0.50 (2)	0.14 (2)	0 (0)
		100	0.60 (6)	0.50 (2)	0.86 (12)	1.00 (4)
15	*Pep-1*	100	0.86 (12)	0.33 (2)	0.40 (4)	0.33 (2)
		102	0.14 (2)	0.67 (4)	0.60 (6)	0.67 (4)
16	*Pep-2*	100	1.00 (10)	1.00 (4)	1.00 (4)	1.00 (6)

CM: Chiang Mai; MS: Mae Hong Son; PB: Phetchaburi

Table 10. Allelic frequencies (allele numbers) observed at 11 isoenzymes 13 loci in adult females of *An. aconitus* Form B (Chiang Mai and Phetchaburi strains) and C (Chiang Mai and Mae Hong Son strains).

No.	Loci	Allele	*An. aconitus* Form			
			B		C	
			CM	PB	CM	MS
1	*Aldox-1*	98	0.07 (4)	0 (0)	0.11 (6)	0 (0)
		100	0.78 (42)	0.67 (4)	0.78 (42)	1.00 (6)
		102	0.15 (8)	0.33 (2)	0.11 (6)	0 (0)
2	*Aldox-2*	98	0 (0)	0.33 (2)	0.10 (4)	0.67 (4)
		100	1.00 (54)	0.67 (4)	0.90 (40)	0.33 (2)
3	*Est-5*	100	0.81 (63)	1.00 (6)	0.83 (43)	0.33 (2)
		104	0.19 (15)	0 (0)	0.17 (9)	0.67 (4)
4	*Fum*	95	0.60 (6)	0 (0)	0.33 (6)	0.33 (2)
		100	0.40 (4)	1.00 (6)	0.67 (12)	0.67 (4)
5	*Hk*	100	1.00 (28)	1.00 (6)	1.00 (12)	1.00 (6)
6	*Ldh-2*	100	1.00 (44)	1.00 (8)	1.00 (42)	1.00 (6)
7	*Mdh-1*	100	1.00 (4)	1.00 (4)	0.75 (3)	1.00 (4)
		105	0 (0)	0(0)	0.25 (1)	0 (0)
8	*Mdh-2*	100	1.00 (4)	1.00 (4)	1.00 (4)	1.00 (4)
9	*Me*	100	1.00 (4)	1.00 (4)	1.00 (4)	1.00 (4)
10	*Gpm*	95	0 (0)	0 (0)	0.04 (1)	0 (0)
		100	0.85 (34)	1.00 (6)	0.88 (23)	1.00 (6)
		105	0.15 (6)	0 (0)	0.08 (2)	0 (0)
11	*Gpi*	100	0.80 (40)	1.00 (6)	0.86 (48)	1.00 (6)
		105	0.20 (10)	0 (0)	0.14 (8)	0 (0)
12	*Xdh*	99	0.10 (2)	0 (0)	0.60 (12)	0 (0)
		100	0.90 (18)	1.00 (6)	0.40 (0)	1.00 (6)
13	*Idh*	95	0 (0)	0.37 (3)	0 (0)	0 (0)
		100	1.00 (12)	0.63 (5)	1.00 (10)	1.00 (6)

CM: Chiang Mai; MS: Mae Hong Son; PB: Phetchaburi

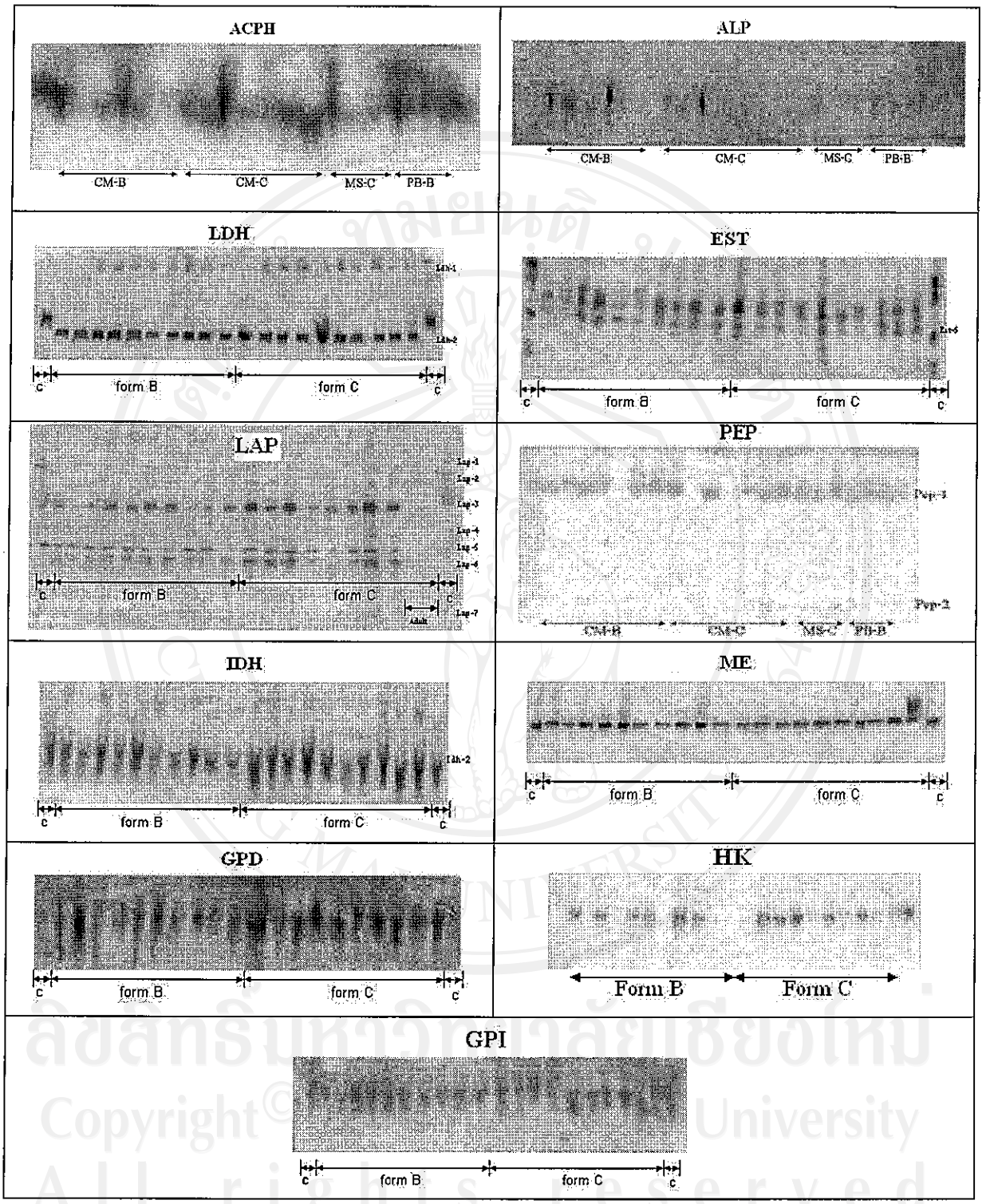

Figure 24. Isoenzyme pattern of ACPH, ALP, EST, GPD, GPI, HK, IDH, LAP, LDH, ME and PEP of 4th instar larva *An. aconitus* Form B and C from Chiang Mai (CM), Mae Hong Son (MS) and Phetchaburi (PB).

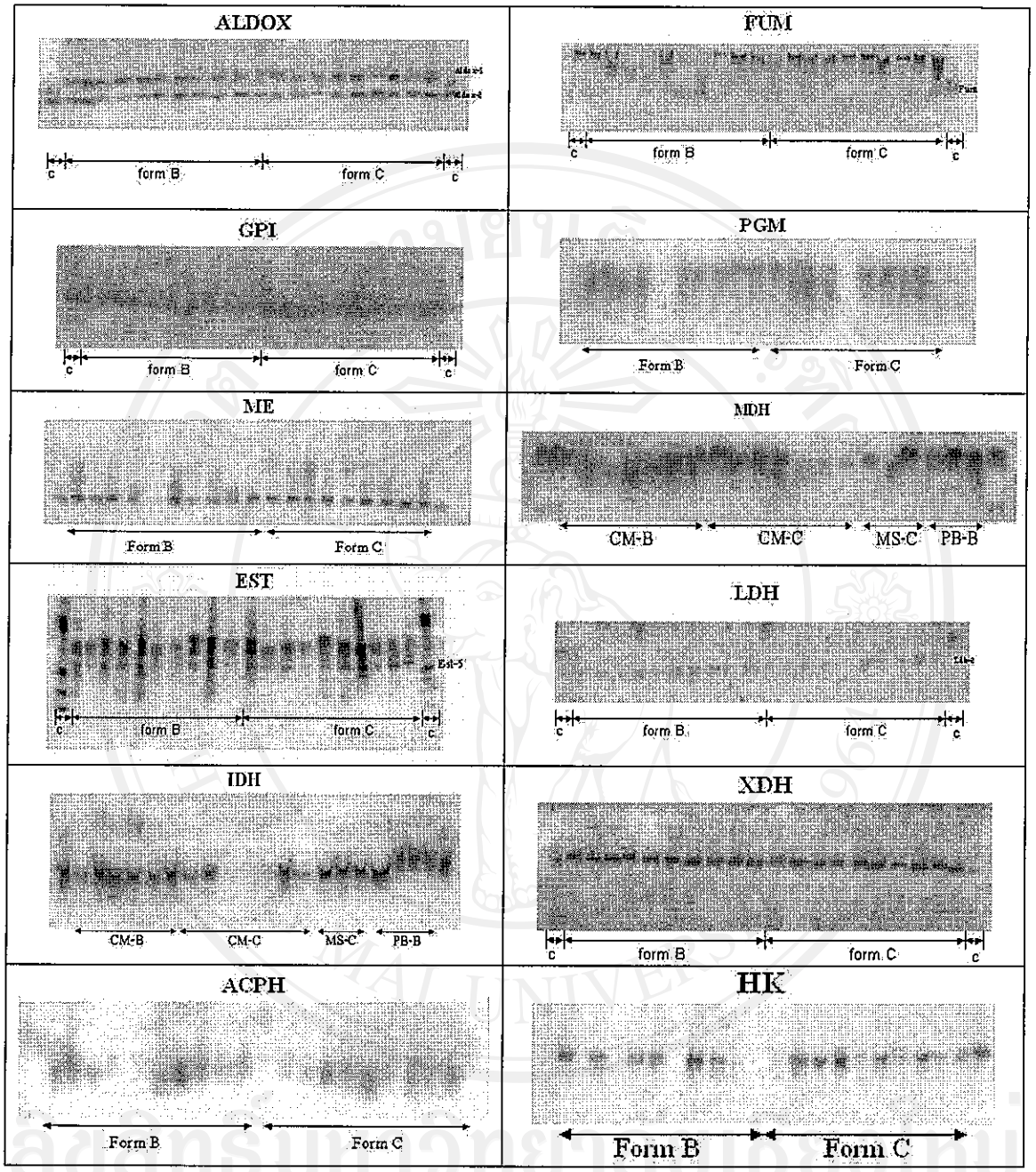

Figure 25. Isoenzyme pattern of ACPH, ALDOX, EST, FUM, GPI, HK, IDH, LDH, MDH, ME, PGM and XDH of adult *An. aconitus* Form B and C from Chiang Mai (CM), Mae Hong Son (MS) and Phetchaburi (PB).

5. Molecular study

5.1 Sequences analysis of ITS2, COI and COII regions

The rDNA ITS2, and mitochondrial COI and COII regions were amplified by PCR from genomic DNA of individual mosquitoes of cytologically identified 12 isolines of *An. aconitus*: half (six isolines) were Form B, and half were Form C. Total sequence lengths (ITS2+COI+COII) of these newly identified *An. aconitus* isolines varied from 1550bp to 1556bp. Intraspecific distances between them ranged from 0.1% to 1.0%. Their geographical origins and Genbank accession numbers are given in Table 11.

Five length polymorphisms were detected from the complete ITS2 sequences of *An. aconitus*, and they varied from 376bp to 381bp in length. The haplotype diversity (Hd) of ITS2 sequences was 1.000. Twenty-four polymorphic nucleotide sites (corresponding to 26 mutations) were identified (excluding all sites with alignment gaps), of which 22 were singletons (92.7%) and only 2 were parsimony informative sites (8.3%) (Figure 26). Intraspecific distances in the *An. aconitus* ranged from 0.0% to 2.9%, whereas the interspecific distances between two species, *An. aconitus* and *An. minimus*, were very high with values of 25.0% to 27.0%.

For compared partial mitochondrial COI and COII sequences, and no length variation was detected: COI and COII contained 506 and 671 nucleotides, respectively. Thirteen and four variable sites were identified from COI and COII sequences, respectively, but all nucleotide polymorphisms were silent. If outgroup sequence of COI (AY423055; Garros *et al.*, 2004) was not considered, only three variation sites remained in the COI alignment (Figure 26).

Table 11. Geographical origin of mosquitoes and their GenBank accession numbers.

Mosquito species	Length of ITS2 (bp)	Symbol of isoline	Region	Genbank accession number			Geographical origin	Reference
				ITS2	COI	COII		
An. aconitus Form B	378	1BPB	ITS2, COI, COII	DQ000241	DQ000253	DQ000265	PB	This study
	379	2BPB	ITS2, COI, COII	DQ000242	DQ000254	DQ000266	PB	This study
	378	3BPB	ITS2, COI, COII	DQ000243	DQ000255	DQ000267	PB	This study
	376	1BCM	ITS2, COI, COII	DQ000244	DQ000256	DQ000268	CM	This study
	381	2BCM	ITS2, COI, COII	DQ000245	DQ000257	DQ000269	CM	This study
	379	3BCM	ITS2, COI, COII	DQ000246	DQ000258	DQ000270	CM	This study
An. aconitus Form C	378	1CCM	ITS2, COI, COII	DQ000247	DQ000259	DQ000271	CM	This study
	379	2CCM	ITS2, COI, COII	DQ000248	DQ000260	DQ000272	CM	This study
	378	3CCM	ITS2, COI, COII	DQ000249	DQ000261	DQ000273	CM	This study
	378	1CMS	ITS2, COI, COII	DQ000250	DQ000262	DQ000274	MS	This study
	377	2CMS	ITS2, COI, COII	DQ000251	DQ000263	DQ000275	MS	This study
	381	3CMS	ITS2, COI, COII	DQ000252	DQ000264	DQ000276	MS	This study
*An. aconitus**	378	Aconi	ITS2	AJ626946	-	-	SL	-
	-	Aconi	COI	-	AY423055	-	-	Garros *et al.* 2004
	-	Aconi	COII	-	-	AJ512744	XM	Chen *et al.* 2003
An. minimus A	373	-	ITS2	AF194504	-	-	KB	Sharpe *et al.* 2000

PB = Phetchaburi, Thailand; CM = Chiang Mai, Thailand; MS = Mae Hong Son, Thailand; SL = Sri Lanka; XM = Xiangming, China; KB= Kanchanaburi, Thailand. *Karyotypic forms were not determined.

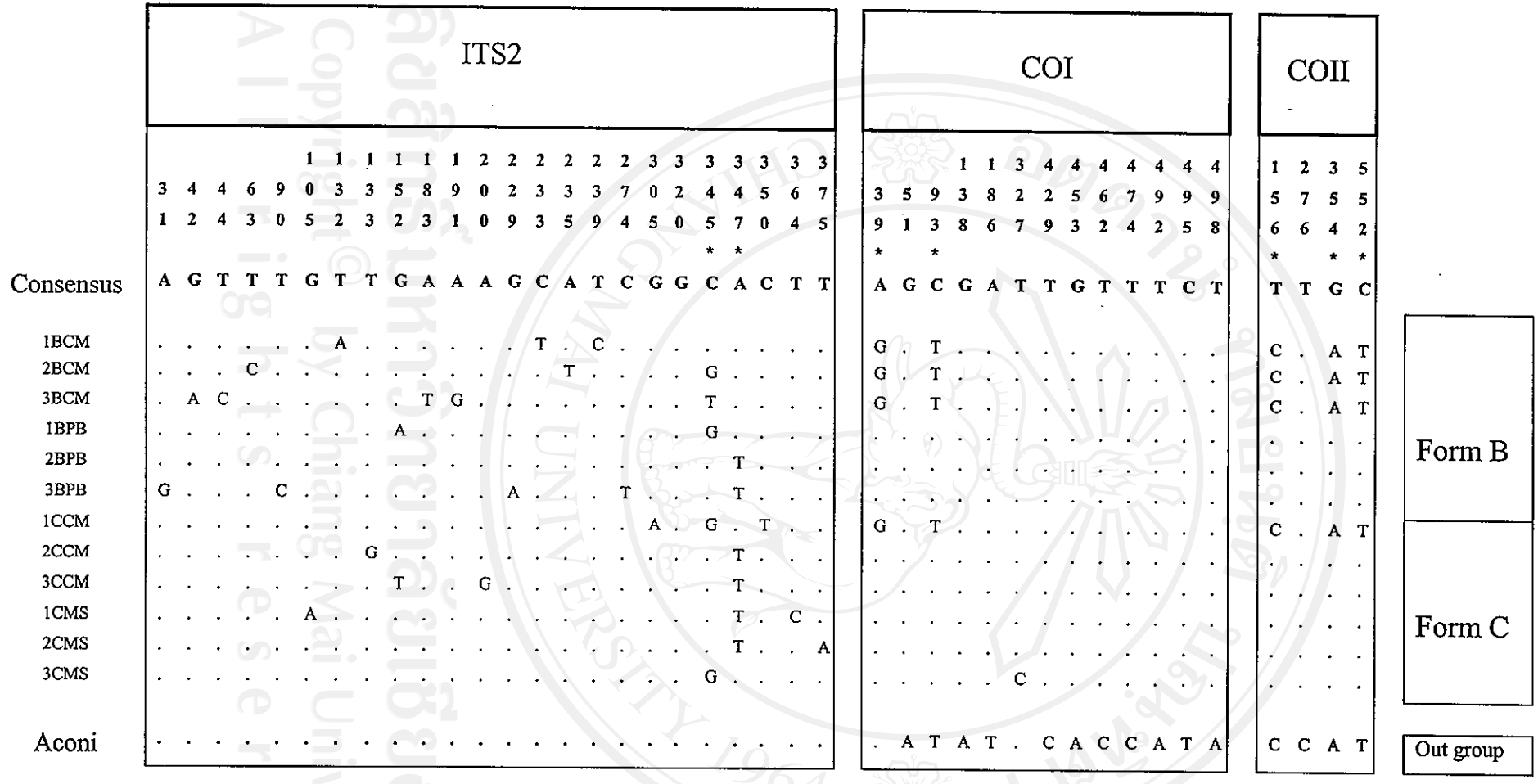

Figure 26. Variable sites in the sequence alignment of the ITS2, COI and COII sequences. Numbering is relative to the alignment. Only those positions differing from the consensus are shown. Indel (insertion or deletion) sites are not shown. An asterisk shows those sites yielding parsimony informative sites. A dot indicates a base pair identical to that of the consensus sequence. Sequence names are defined in Table10.

To explore the conflict between data sets, pairwise incongruence was estimated using a partition homogeneity test (Farris *et al.*, 1994), which indicated that the data sets from these three distinct gene regions were heterogeneous (P = 0.24). Therefore the data sets should not be combined for analysis. To measure the nucleotide divergences between isoline groups of *An. aconitus* Form B and Form C, used only ITS2 sequences because most of informative variations were in ITS2 (24 out of 30 variable sites: 80%). Summary of polymorphism within- and between-isoline groups of Form B and Form C is given in Table 12. The average nucleotide diversity (p) among Form B isolines (0.01667) was slightly greater than among those of Form C (0.00993). The genetic differentiation between two groups was very low as measured by d_{xy} (0.01322). In fact, there was no fixed variation between two groups, and most of variable sites were singletons. The lack of genetic differentiation between two groups was also supported by the result of the permutation test (Hudson *et al.*, 1992) (P = 0.62 for K_s^* estimator).

Table 12. Nucleotide polymorphism within and between isoline sequences of *An. aconitus* Form B and C.

	Form B	Form C	Form B vs Form C
Sample size	6	6	12
Fixed variation	0	0	0
S (singletons)	17 (15)	10 (8)	24 (22)
k	6.263	3.733	3.972
p	0.01667	0.00993	-
d_{xy}	-	-	0.01322

S: number of segregating site; k: average number of pairwise nucleotide differences; p: nucleotide diversity; d_{xy}: average number of nucleotide substitutions per site between groups.

6. Hybridization study

Details of hatchability, pupation and emergences of parental, reciprocal, and back-crosses among four isolines of three strains of *An. aconitus* Form B and C are displayed in Table 13. Observations on the hatchability, pupation, emergence, and adult sex-ratio of parental, reciprocal and back-crosses among four isolines that represented two karyotypic forms, revealed that all crosses yielded viable progenies, and no evidence of genetic incompatibility was observed between *An. aconitus* Form B and C. The hatchability, pupation, emergence rates, and adult female/male ratio of parental; reciprocal; and back-crosses were 66.85-86.75%, 81.16-91.87%, 94.39-97.30% and 0.77-1.40; 70.89-87.10%, 82.96-92.86%, 86.72-100% and 0.67-1.35; 70.90-91.03%, 77.86-97.89%, 93.17-100% and 0.59-1.52, respectively. The salivary gland polytene chromosomes of the 4th instar larvae from all crosses showed complete synapsis along the whole length of all autosomes and the X- chromosome (Figure 27).

Table 13. Cross mating among isolines of *An. aconitus* Form B and C.

Cross	Total egg (No.)*	Embryonation rate**	No. hatched (%)	No. pupation (%)	No. emergence (%)	No. females and males from total emergence (%)		Sex ratio Female/Male
Female x Male						Female	Male	
Parental crosses								
BC x BC	151 (62, 89)	90	131 (86.75)	107 (81.68)	101 (94.39)	59 (58.42)	42 (41.58)	1.40
BP x BP	197 (92,105)	88	166 (84.26)	148 (89.16)	144 (97.30)	66 (45.83)	78 (54.17)	0.85
CC x CC	184 (86, 98)	72	123 (66.85)	113 (91.87)	109 (96.46)	59 (54.13)	50 (45.87)	1.18
CM x CM	170 (79, 91)	89	138 (81.18)	112 (81.16)	108 (96.43)	47 (43.52)	61 (56.48)	0.77
Reciprocal crosses								
BC x BP	169 (55, 114)	89	139 (82.25)	128 (92.09)	111 (86.72)	46 (41.44)	65 (58.56)	0.71
BP x BC	217 (65, 152)	90	189 (87.10)	166 (87.83)	151 (90.96)	77 (50.99)	74 (49.01)	1.04
BC x CC	159 (77, 82)	80	121 (76.10)	110 (90.91)	107 (97.27)	51 (47.66)	56 (52.34)	0.91
CC x BC	162 (67, 95)	89	135 (83.33)	112 (82.96)	112 (100)	45 (40.18)	67 (59.82)	0.67
BC x CM	158 (61, 97)	75	112 (70.89)	104 (92.86)	104 (100)	43 (41.35)	61 (58.65)	0.70
CM x BC	164 (81, 83)	86	136 (82.93)	125 (91.91)	120 (96.00)	69 (57.50)	51 (42.50)	1.35
Back crosses								
(BC x BP)F_1 x BP	156 (57, 99)	94	142 (91.03)	139 (97.89)	136 (97.84)	81 (59.56)	55 (40.44)	1.47
BC x (BC x BP)F_1	186 (88, 98)	88	151 (81.18)	128 (84.77)	126 (98.44)	76 (60.32)	50 (39.68)	1.52
(BP x BC)F_1 x BC	189 (94, 95)	76	134 (70.90)	121 (90.30)	121 (100)	52 (42.98)	69 (57.02)	0.75
BP x (BP x BC)F_1	162 (67, 95)	88	133 (82.10)	124 (93.23)	119 (95.97)	44 (36.97)	75 (63.03)	0.59
(BC x CC)F_1 x CC	170 (79, 91)	79	122 (71.76)	115 (94.26)	113 (98.26)	68 (60.18)	45 (39.82)	1.51
BC x (BC x CC)F_1	181 (83, 98)	89	147 (81.22)	137 (93.20)	137 (100)	71 (51.82)	66 (48.18)	1.08
(CC x BC)F_1 x BC	210 (65, 145)	92	181 (86.19)	157 (86.74)	157 (100)	88 (56.05)	69 (43.95)	1.28
CC x (CC x BC)F_1	160 (58, 102)	87	131 (81.88)	102 (77.86)	102 (100)	53 (51.96)	49 (48.04)	1.08
(BC x CM)F_1 x CM	165 (79, 86)	91	144 (87.27)	128 (88.89)	128 (100)	62 (48.44)	66 (51.56)	0.94
BC x (BC x CM)F_1	256 (84, 172)	88	220 (85.94)	205 (93.18)	191 (93.17)	84 (43.98)	107 (56.02)	0.79
(CM x BC)F_1 x BC	163 (67, 96)	74	116 (71.17)	91 (78.45)	89 (97.80)	40 (44.94)	49 (55.06)	0.82
CM x (CM x BC)F_1	169 (76, 93)	81	135 (79.88)	127 (94.07)	122 (96.06)	59 (48.36)	63 (51.64)	0.94

BC: *An. aconitus* Form B (Chiang Mai strain); BP: *An. aconitus* Form B (Phetchaburi strain); CC: *An. aconitus* Form C (Chiang Mai strain); CM: *An. aconitus* Form C (Mae Hong Son strain), *Two selective egg-batches of inseminated females from each cross, **Dissection from one hundred eggs.

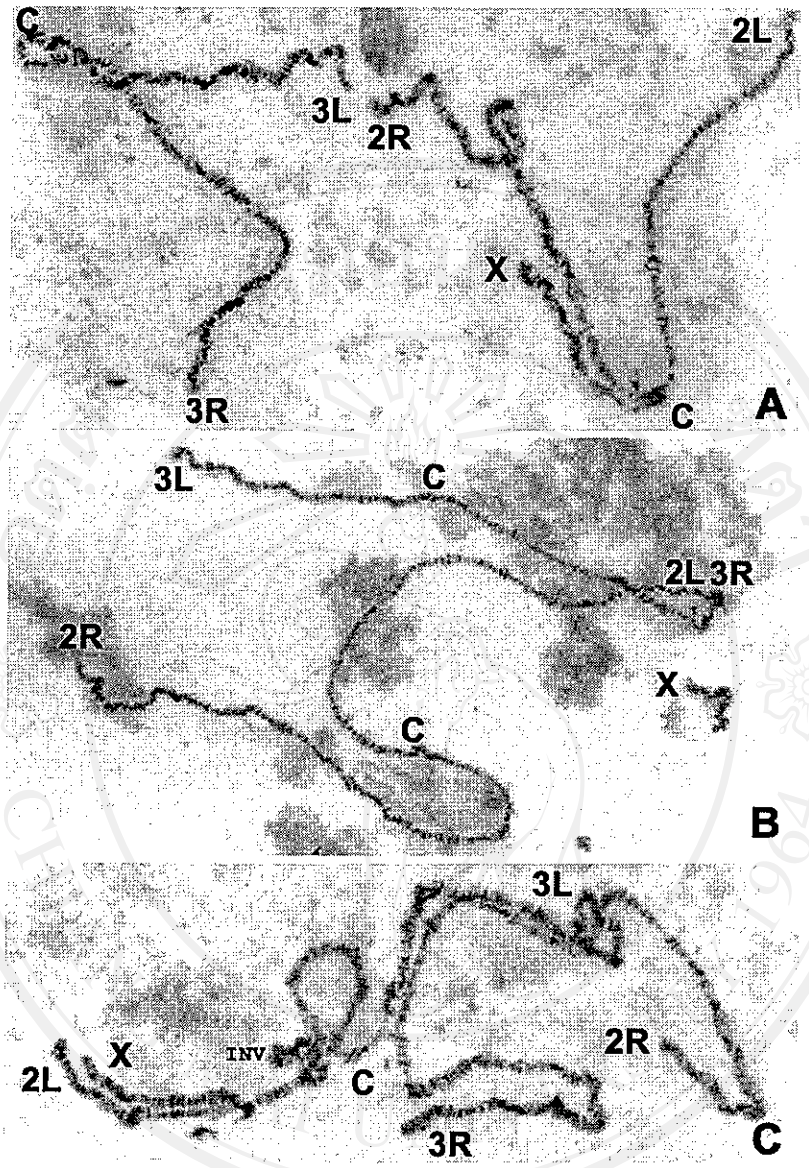

Figure 27. Salivary gland polytene chromosome of F_1-hybrid 4th instar larvae of *An. aconitus*: (A) Form B female (Chiang Mai strain) x Form B male (Phetchaburi strain), (B) Form B female (Chiang Mai strain) x Form C male (Chiang Mai strain), (C) Form B female (Chiang Mai strain) x Form C male (Mae Hong Son strain). All the crosses yielded complete synapsis in all arms, except floating and heterozygous inversion (INV) on 2L (C), which was found in only one preparation from the F_1-hybrid 4th instar larvae of Form B female (Chiang Mai strain) x Form C male (Mae Hong Son strain).

7. Malarial susceptibility test

7.1 Oocyst rates of *An. dirus* B, *An. minimus* A and C, and *An. aconitus* Form B and C.

Details of oocyst rates are shown in Table 14. Observations on dissected midguts 8 days after feeding revealed that *An. aconitus* Form B were susceptible to both *P. falciparum* and *P. vivax*, and Form C was susceptible to *P. vivax*. The 100% oocyst rates and 5.22-126.18 average number of oocysts per infected midgut obtained from *An. dirus* B, the outgroup control mosquito-vector, indicated the all feedings were conditional experiments, which reflected on the proper density and maturity of infective gametocytes in infected blood.

In the experimental feedings of *P. falciparum*, the oocyst rates and average number of oocysts per infected midgut of *An. aconitus* Form B (Chiang Mai and Phetchaburi strains) did not differ significantly ($P > 0.05$) from the ingroup control-vector, *An. minimus* A. Similar results also were obtained from statistical analysis of the oocyst rates and average number of oocysts per infected midgut between *An. aconitus* Form B strains from Chiang Mai and Phetchaburi provinces.

In the experimental feedings of *P. vivax*, mostly, the oocyst rates and average number of oocysts per infected midgut of *An. aconitus* Form B (Chiang Mai and Phetchaburi strains) and C (Chiang Mai and Mae Hong Son strains) did not differ significantly ($P > 0.05$) from *An. minimus* A and C, except the average number of oocysts per infected midgut of *An. aconitus* Form C (Chiang Mai strain: experiment 1) was significantly less than that in *An. minimus* A, and Form C (Mae Hong Son strain: experiment 2) was significantly greater than that in the *An. minimus* A. Similar results also were recovered from statistical analysis of the oocyst rates and average number

of oocysts per infected midgut between *An. aconitus* Form B (Chiang Mai strain) and C (Chiang Mai and Mae Hong Son strains) in experiment 1 and 2, except for only the average number of oocysts per infected midgut of *An. aconitus* Form C (Mae Hong Son strain) was significantly greater than that in the Form B (Chiang Mai strain) in experiment 2.

Table 14. The oocyst rates of *An. dirus* B, *An. minimus* A and C and *An. aconitus* Form B and C after feeding on blood containing gametocytes of *P. falciparum* and *P. vivax*, all dissected 8 days after feeding.

Malaria species	Mosquito species						
	An. dirus B	*An. minimus*		*An. aconitus* Form			
		A	C	B		C	
				CM	PB	CM	MS
P. falciparum							
Oocyst rate (No.)	100 (20/20)	91.67 (11/12)	ND	62.50 (5/8) NS	80.00 (8/10) NS	ND	ND
Average No. oocysts per Infected midgut (range)	84.75 ± 45.53 (19-182)	18.64 ± 22.61 (1-81)	ND	31.40 ± 21.85 NS (2-35)	19.63 ± 25.14 NS (1-79)		
P. vivax							
Experiment 1							
Oocyst rate (No.)	100 (7/7)	100 (5/5)	ND	100 (5/5)	ND	60.00 (3/5) NS	ND
Average No. oocysts per Infected midgut (range)	69.71 ± 26.82 (39-118)	18.00 ± 6.93 (11-27)	ND	10.00 ± 6.04 (4-19)	ND	4.33 ± 4.93 * (1-10)	ND
Experiment 2							
Oocyst rate (No.)	90.00 (9/10)	83.33 (5/6)	ND	66.67 (4/6) NS	ND	ND	66.67 (4/6) NS
Average No. oocysts per Infected midgut (range)	5.22 ± 3.73 (1-11)	2.00 ± 1.41 (1-4)	ND	1.00 ± 0.00 (1)	ND	ND	6.00 ± 3.46 * (3-9)
Experiment 3							
Oocyst rate (No.)	100 (11/11)	81.82 (9/11)	50.00 (5/10) NS	ND	50.00 (2/4) NS	ND	ND
Average No. oocysts per Infected midgut (range)	126.18 ± 55.92 (34-223)	22.78 ± 15.18 (2-54)	7.80 ± 8.23 NS (1-22)	ND	19.50 ± 12.02 NS (11-28)	ND	ND

Mosquito strain; CM: Chiang Mai, MS: Mae Hong Son, PB: Phetchaburi; Oocyst rate: NS, $P > 0.05$, *, $P < 0.05$ (Fisher exact test); Average No. oocysts per infected midgut: NS, $P > 0.05$, * , $P < 0.05$ (t-test, two-sided); ND: not done.

7.2 Oocyst and sporozoite rates of *An. dirus* B, *An. minimus* A and C, and *An. aconitus* Form B and C.

Details of oocyst and sporozoite rates are shown in Table 15. The dissection of midgut of *An. dirus* B, *An. minimus* A and C, and all strains of *An. aconitus* Form B and C 12 days after feeding on blood containing *P. falciparum* and *P. vivax* gametocytes revealed that the oocyst rates were 95% (*An. aconitus* Form B: Phetchaburi strain), 96.30% (*An. aconitus* Form B: Chiang Mai strain), 100% (*An. minimus* A), and 100% (*An. dirus* B), for *P. falciparum*, and 14.28-75% (all strains of *An. aconitus* Form B and C), 39.13% (*An. minimus* C), 11.11-100% (*An. minimus* A) and 15.79-100% (*An. dirus* B) for *P. vivax*. Statistical analyses of the oocyst rates among the ingroup control mosquito-vectors, *An. minimus* A and C, and all strains of *An. aconitus* Form B and C were not done because at this period (12 days of postblood meal) the mature oocysts from the midgut of the control vectors ruptured and yielded unreliable results. Nonetheless, the satisfactory percentages of oocyst rates obtained from both outgroup and ingroup control-vectors were confirmed the conditional experiments.

The dissection of salivary glands 12 days after feeding demonstrated that *An. aconitus* Form B strains from Chiang Mai and Phetchaburi provinces were efficiently potential vectors for *P. falciparum*, and Form B strains from Chiang Mai and Phetchaburi provinces and Form C strains from Chiang Mai and Mae Hong Son provinces were the efficiently potential vectors for *P. vivax* when compared to the ingroup control-vectors, *An. minimus* A and C. Comparative statistical analyses of sporozoite rates among *An. minimus* A and C, and four strains of *An. aconitus* Form B and C of all experiments exhibited no significant differences ($P > 0.05$), except only

An. aconitus Form B (Phetchaburi strain) differed significantly ($P < 0.05$) in the experimental feeding of *P. falciparum.*

Table 15. The oocyst and sporozoite rates of *An. dirus* B, *An. minimus* A and C and *An. aconitus* Form B and C after feeding on blood containing gametocytes of *P. falciparum* and *P. vivax*, all dissected 12 days after feeding.

Malaria species	Mosquito species						
	An. dirus B	*An. minimus*		*An. aconitus* Form			
		A	C	B		C	
				CM	PB	CM	MS
P. falciparum							
Oocyst rate (No.)	100 (23/23)	100 (11/11)	ND	96.30 (26/27)	95.00 (19/20)	ND	ND
Average No. oocysts per	85.00 ± 26.41	5.45 ± 3.86	ND	13.35 ± 15.60	28.58 ± 28.42	ND	ND
Infected midgut (range)	(39-145)	(1-15)		(1-54)	(2-90)		
Sporozoite rate (No.)	95.65 (22/23)	100 (11/11)	ND	70.37 (19/27) NS	45.00 (9/20) *	ND	ND
P. vivax							
Experiment 1							
Oocyst rate (No.)	100 (4/4)	100 (2/2)	ND	ND	ND	100 (4/4)	ND
Average No. oocysts per	28.00 ± 25.07	5.50 ± 4.95	ND	ND	ND	9.75 ± 4.03	ND
Infected midgut (range)	(6-64)	(2-9)				(5-14)	
Sporozoite rate (No.)	100 (4/4)	100 (2/2)	ND	ND	ND	100 (4/4)	ND
Experiment 2							
Oocyst rate (No.)	15.79 (3/19)	11.11 (1/9)	ND	16.67 (2/12)	ND	ND	14.28 (2/14)
Average No. oocysts per	1.33 ± 0.58	1.00 ± 0.00	ND	2.00 ± 1.41	ND	ND	1.00 ± 0.00
Infected midgut (range)	(1-2)	(1)		(1-3)			(1)
Sporozoite rate (No.)	80.00 (16/20)	33.33 (3/9)	ND	16.67 (2/12) NS	ND	ND	14.28 (2/14) NS
Experiment 3							
Oocyst rate (No.)	100 (17/17)	66.67 (12/18)	39.13 (9/23)	ND	75.00 (9/12)	ND	ND
Average No. oocysts per	33.53 ± 20.12	2.92 ± 1.24	2.89 ± 1.83	ND	2.89 ± 2.15	ND	ND
Infected midgut (range)	(7-77)	(1-5)	(1-6)		(1-7)		
Sporozoite rate (No.)	100 (17/17)	77.78 (14/18)	52.17 (12/23) NS	ND	66.67 (8/12) NS	ND	ND

Mosquito strain; CM: Chiang Mai, MS: Mae Hong Son, PB: Phetchaburi; Sporozoite rate: NS, $P > 0.05$, *, $P < 0.05$ (Fisher exact test, χ^2-test for only experiment 3); ND: not done.

Another interesting point in the present study is the sporozoite-like crystal found in the median lobe of the salivary glands of both *An. aconitus* Form B and C, *i.e.*, Form B: Chiang Mai strain 3.70% (1/27), Phetchaburi strain 20% (4/20) (experimental feeding on *P. falciparum*); Form C: Mae Hong Son strain 28.57% (4/14) (experimental feeding on *P. vivax*). The sporozoite-like crystal rather resembles a true sporozoite, particularly, when it is inside a non-squashed salivary glands. The latter has regular spindle-shaped, while the former has irregular, long or short with blunt or tapered end(s) (Figure 28). It was stable in 0.85% normal saline solution for at least half an hour and after that the dissolve of the crystal could be obviously seen, and could be easily distinguished from the true sporozoite.

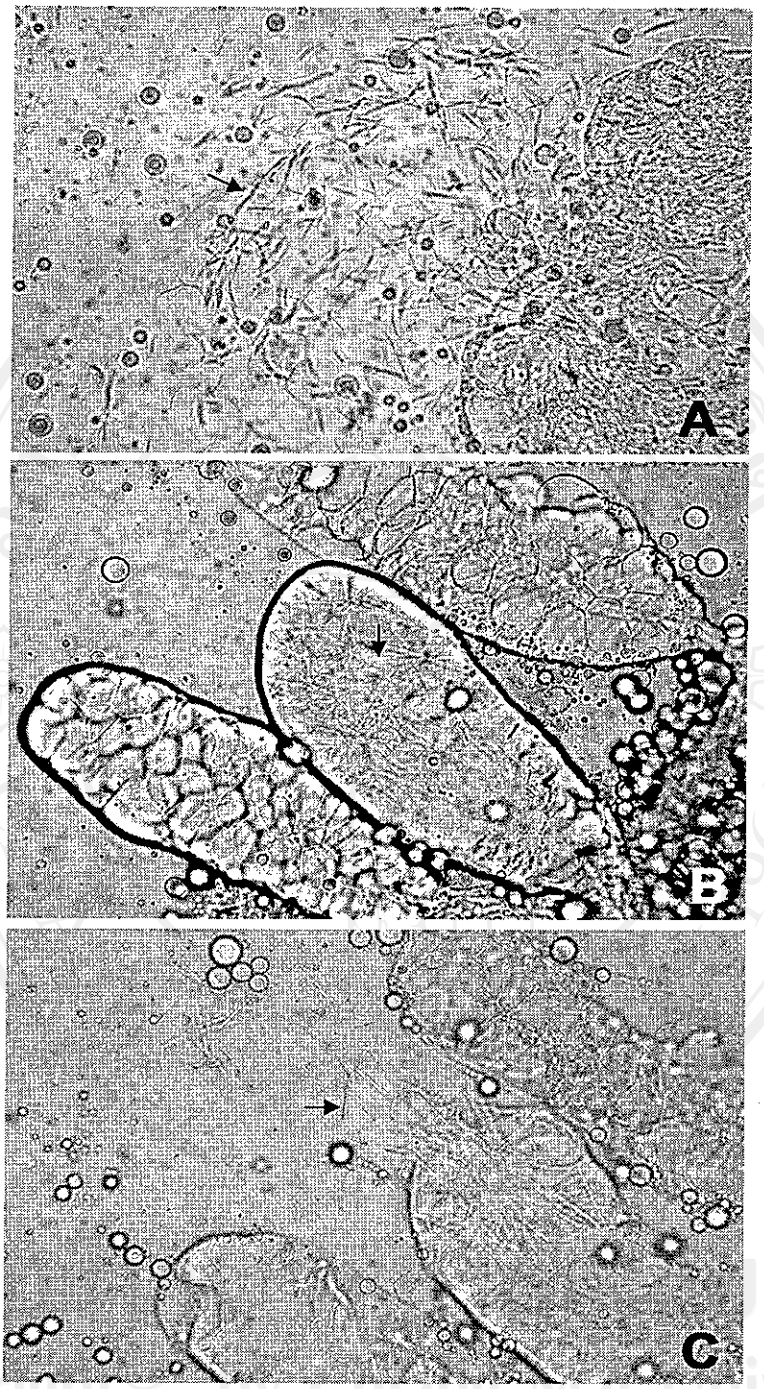

Figure 28. Salivary glands of *An. aconitus* Form B. (A) Showing free flow *P. vivax* sporozoites from the squashed salivary glands. Note, the regular spindle-shaped sporozoites (small arrow). (B) Showing sporozoite-like crystals inside the median lobe of salivary glands (small arrow). (C) Showing free flow sporozoite-like crystals from the squashed salivary glands. Note, the irregular, long or short, crystals with blunt or tapered end(s) (small arrow).